

# THERMODYNAMIC ANALYSIS PROCEDURES AT THE NATIONAL SEVERE STORMS FORECAST CENTER

Charles A. Doswell III, Joseph T. Schaefer and Donald W. McCann  
National Severe Storms Forecast Center  
Kansas City, Missouri 64106-2877

Thomas W. Schlatter  
PROFS Program Office  
Environmental Research Laboratories  
Boulder, Colorado 80303

Hermann B. Wobus  
Old Dominion University  
Norfolk, Virginia 235088512

## 1. INTRODUCTION

Thermodynamic analysis is a keystone of convective forecasting. However, owing to the implicit dependence of the various thermodynamic relationships, approximations are required for automated evaluation. This, coupled with the complex charts needed for sounding presentation, has led to the development of myriad convective indices (e.g., David and Smith, 1971).

Recently, major revisions in the rawinsonde analysis algorithms used operationally at NSSFC were undertaken. These changes were motivated both by the availability of more accurate and efficient approximations to the intractable moist thermodynamic relationships and by a desire to put forecast indices on a more physical (i.e., less empirical) basis. The revised algorithms are presented, and several of the revised indices are examined.

## 2. EQUIVALENT HEAT ENERGY OF MOISTURE

A basic parameter useful in thermodynamic analysis is the pseudo-wet bulb potential temperature\* difference between two hypothetical air parcels, each having the same temperature and pressure, but one is saturated and the other absolutely dry. To express this formally for a parcel with temperature (T) and pressure (p), define

- $\theta_w$  as the wet bulb potential temperature,
- $\theta_M$  as  $\theta_w$  for saturated conditions at (T,p),
- $\theta_A$  as  $\theta_w$  for dry conditions (mixing ratio equal to zero) at (T,p).

The equation

$$W(T) = \theta_M - \theta_A \quad (1)$$

defines the parameter of interest, W - the "Wobus function".

\*Since the distinction implied by "pseudo" is so small as to be of only esoteric interest, the prefix will not be used. All thermodynamic processes are to be understood as "pseudo". Also, pseudo-adiabats will be referred to as moist adiabats.

To examine this parameter, consider the point (T,p) in Fig. 1. The moist adiabat through this point is simply  $\theta_M$ . However, this point can also be uniquely related to the moist adiabat which, at very high levels, becomes asymptotic to the dry adiabat through (T,p). Conceptually, a parcel at (T,p) can be lifted dry adiabatically to the juncture only if it is absolutely dry (vapor pressure equals zero). Then as such a parcel is forced to descend while absorbing enough water vapor to maintain saturation, its temperature trace will follow this moist adiabat, along which the wet bulb potential temperature  $\theta_A$  is constant. Once back at p, the parcel has a temperature  $T_A$ .  $\theta_A$  may be viewed as the wet bulb potential temperature of a perfectly dry parcel at (T,p). W is the difference in degrees Celcius between  $\theta_M$  and  $\theta_A$ . It is proportional to the heat that would be imparted to a saturated parcel at  $T_A$  if all of its water vapor were to be condensed. Since the amount of water vapor needed to saturate a parcel is dependent only upon its temperature, it is obvious that even though  $\theta_M$  and  $\theta_A$  are functions of pressure and temperature, W is a function only of temperature.

Several thermodynamic quantities can be functionally related to this parameter. If p is 1000 mb and the parcel is absolutely dry, its temperature (T) is the same as its equivalent potential temperature ( $\theta_e$ ) and its wet bulb potential temperature ( $\theta_w$ ) is  $\theta_A$ . Therefore, it is seen that

$$W(\theta_e) = \theta_e - \theta_w \quad (2)$$

Also at 1000 mb, T is a potential temperature ( $\theta$ ) and the relationship

$$W(\theta) = \theta - \theta_A \quad (3)$$

holds. Similarly, at condensation conditions (T,P) = (T<sub>c</sub>, P<sub>c</sub>),  $\theta_M = \theta_w$  and

$$W(T_c) = \theta_w - \theta_A \quad (4)$$

Combining (3) and (4), the wet bulb potential temperature of a parcel is found to be simply

$$\Theta_W = \Theta - W(\Theta) + W(T_C). \quad (5)$$

When diagnosing conditional instability,  $\Theta_M$  is needed. Combining (1) and (3) gives

$$\Theta_M = \Theta - W(\Theta) + W(T), \quad (6)$$

the formulation required.

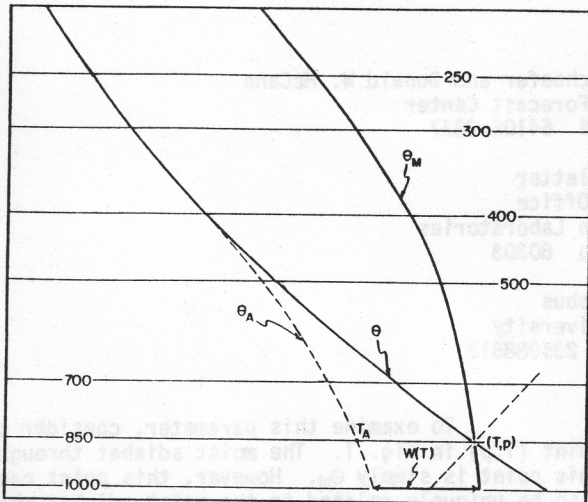


Fig. 1. Schematic showing the relevant curves for the Wobus function,  $W(T)$ . The labelling for the curves is as discussed in the text, while the unlabelled dashed line is the (skewed) isotherm through the point  $(T, p)$ .

Computation of  $W$  is rather simple when one considers (2). Values of the right-hand side are obtainable from Table 78 of the Smithsonian Meteorological Tables (List, 1966), and a polynomial is fitted to the inverse of the data (e.g., Hastings, 1955). Two different curves are used, one for  $T$  greater than  $20^\circ\text{C}$  and one for  $T$  cooler less than  $20^\circ\text{C}$  (Table 1). This curve fit allows for the direct, non-iterative calculation of  $\Theta_W$ ,  $\Theta_M$  and  $\Theta_A$ . These quantities are also directly (although non-linearly) related to moist static energy (Kreitzberg, 1964; Darkow and Livingston, 1973).

TABLE 1  
ALGORITHM TO COMPUTE  $W$  FUNCTION

```

FUNCTION WOBF(T)
  COMPUTE BY DOUBLE ASYMPTOTIC APPROXIMATION
  CONSIDER SEPARATELY IF .GT. OR .LE. 20 DEG.
  CENT. FOR ALL TEMPS...THETW=THETA-WOBF(THETA)+WOBF(TEMPCON)
  CENT. FOR ALL TEMPS...THETM=THETA-WOBF(THETA)+WOBF(TEMP)
  X=T-20.0
  IF(X) 10,10,20
  10 CONTINUE
  CURVE FIT FOR COOL TEMPERATURE RANGE
  POL=1.000+X*(-8.8416605E-3
  A=X*(1.4714143E-4+X*(-9.6719890E-7
  B=X*(-3.2607217E-8+X*(-3.8598073E-10))))
  POL=POL*POL
  WOBF=15.130/(POL*POL)
  RETURN
  20 CONTINUE
  CURVE FIT FOR WARMER TEMPERATURES
  POL=1.000+X*(3.6182989E-3
  1+X*(-1.3603273E-5+X*(4.9618922E-7
  2+X*(-6.1059365E-9+X*(3.9401551E-11
  3+X*(-1.2588129E-13+X*(1.6688280E-16))))))
  POL=POL*POL
  WOBF=29.930/(POL*POL)+0.9600*X-14.800
  RETURN
END
  
```

To calculate the wet bulb potential temperature, the lifted condensation temperature ( $T_C$ ) must be obtained. The formula to compute this temperature is well-known (e.g., Berry, Bollay and Beers, 1945). However, owing to the

implicitness of the relationship, either iterative solutions (e.g., Stackpole, 1967) theoretical approximations (e.g., Inman, 1969), or empirical fits (e.g., Barnes, 1968) must be employed. In order to combine accuracy with efficiency, the latter approach is used here.

From tabulated data (List, 1966), it can be seen that for a given temperature, there is a quasi-quadratic relationship between the dew point depression and  $T_C$ . Also, for a given dew point depression, there is an almost linear fit between  $T$  and  $T_C$ . These facts are combined via regression into an empirical algorithm (Table 2). Equation 5 can now be solved for  $\Theta_W$ .

TABLE 2  
ALGORITHM TO COMPUTE CONDENSATION TEMPERATURE

```

FUNCTION TCONOF(TEMP,DEWPT)
  COMPUTES CONDENSATION TEMPERATURE (DEGREES CENT) BY LIFTING
  S=TEMP-DEWPT
  CONSIDER TEMP AND DEWTEMP TO BE LIKE UNITS (C OR K)
  T=TEMP
  IF(100.0-TEMP)4,5,5
  4 T=TEMP-273.16
  COMPUTE CURVE FIT IN MOST EFFICIENT MANNER
  5 DLT=S*(1.2185+0.001278*T+S*(-0.002190+11.73E-6*S-5.20E-6*T))
  TCONOF=T-DLT
  RETURN
END
  
```

With a routine to calculate  $\Theta_W$  available, determination of a parcel's temperature as it is lifted along a moist adiabat to any specified pressure level is quite simple. The computational procedure (Table 3) corrects iteratively the difference between the  $\Theta_W$  implied by a "guess" temperature and the known  $\Theta_W$  of the moist adiabat. Convergence is very rapid: less than  $0.1^\circ\text{C}$  differences can be obtained typically within three iterations. It should be noted that values obtained are dependent upon the ratio of the gas constant and the specific heat capacity at constant pressure used in the potential temperature calculation. We use a ratio of  $2/7$  as dictated by statistical mechanics, while the Smithsonian Tables (List, 1966) are based upon a slightly different value.

TABLE 3  
ALGORITHM TO LIFT PARCEL ALONG PSEUDO-ADIABAT

```

FUNCTION SATLFT(THM,P)
  COMPUTES TEMPERATURE(DEC C) WHERE THETA MOIST (DEC,C) CROSSES P(MB)
  CONSIDER THE EXPONENTIAL FOR POTENTIAL TEMPERATURE AS ROCP
  ROCP=0.28571428
  IF(ABS(P-1000.0)-0.0010) 100,100,200
  100 SATLFT=THM
  RETURN
  200 PWRP=(P/1000.0)**ROCP
  COMPUTE TEMPERATURE OF DRY ADIABATIC LIFT FOR FIRST GUESS
  TONE=(THM+273.16)*PWRP-273.16
  CONSIDER PSEUDO-ADIABAT, EW1, THROUGH TONE AT P.
  COMPUTE EONE=EW1-THM
  EONE=WOBF(TONE)-WOBF(THM)
  RATE=1.0
  GO TO 300
  300 CONTINUE
  CONTRIBUTION TO ITERATION IS CHANGE IN T
  CORRESPONDING TO CHANGE IN E
  RATE=(TTWO-TONE)/(ETWO-EONE)
  TONE=TTWO
  EONE=ETWO
  330 CONTINUE
  COMPUTE ESTIMATED SATLIFT,TTWO
  TTWO=TONE-EONE*RATE
  CONSIDER PSEUDO-ADIABAT, EW2, THROUGH TTWO AT P.
  COMPUTE ETWO=EW2-THM
  ETWO=(TTWO+273.16)/PWRP-273.16
  ETWO=ETWO+WOBF(TTWO)-WOBF(ETWO)-THM
  CORRECTION TO TTWO IS EOR
  EOR=ETWO*RATE
  IF(ABS(EOR)-0.1000) 400,400,300
  400 SATLFT=TTWO-EOR
  RETURN
END
  
```

Since the lift is considered to occur in one step, this routine differs markedly from most lifted temperature algorithms which use very small vertical steps. Also, it is noteworthy that



only one exponentiation is required. Thus, this program is more computationally efficient than one presented by Stackpole (1967) which follows similar logic but considers  $\Theta_e$  instead of  $\Theta_w$ , and requires one exponentiation per iteration. These are exact routines and contrast with those of Prosser and Foster (1966) who compute lifted parcel temperatures by linear interpolation between known temperatures along two specified moist adiabats. Although computationally fast, their technique is subject to considerable error.

### 3. OTHER THERMODYNAMIC APPROXIMATIONS

Perhaps the most basic approximation needed for atmospheric thermodynamics is one to compute accurately and efficiently the saturation vapor pressure with respect to liquid water. As noted by Lowe (1977), many techniques exist. Typically, the approximation is in the form of an exponential or a polynomial fit to empirical data. The algorithm we employ takes advantage of the quasi-exponential relationship of the saturation vapor pressure to temperature and fits a polynomial to the inverse of the data. As indicated in Hastings (1955) this type fit is quite efficient and a seventy-second order polynomial with only ten coefficients and twelve multiplications can be obtained (Table 4). Errors are not greater than .02% for temperatures between -50°C and 100°C.

TABLE 4  
ALGORITHM TO COMPUTE SATURATION VAPOR PRESSURE  
WITH RESPECT TO WATER

```

FUNCTION VAPFW(T)
COMPUTE SATURATION VAPOR PRESSURE OVER WATER, VAPFW, IN MBS.
CONSIDER T(TEMPERATURE) IN DEGREES C
X=T
IF(100.0-X) 3,4,4
X=X-273.16
3 CURVE FIT FOR RANGE -50 < T < 100
4 POL = 0.99999683 E-00 + X*(-0.90826951 E-02 +
1 X*(0.78736169 E-04 + X*(-0.61117958 E-06 +
2 X*(0.43884187 E-08 + X*(-0.29883885 E-10 +
3 X*(0.21874425 E-12 + X*(-0.17892321 E-14 +
4 X*(0.11112018 E-16 + X*(-0.30994571 E-19))))))
POL=POL*POL
POL=POL*POL
VAPFW=6.107800/(POL*POL)
RETURN
END

```

Knowledge of the vapor pressure dependence can be inverted to give the relationship of the dew point temperature to the vapor pressure. Calculation consists of inverting Tetens's formula (e.g., Murray, 1967) and calculating an iterative

correction (to the accuracy desired) based on the local derivative of dew point temperatures with respect to vapor pressure (Table 5). Bolton (1980) presents a similar inversion but does not include the fine tuning via iteration.

The final algorithm considered converts the dew point temperature at a given pressure to a mixing ratio. This determination is more complicated than the text book equation (e.g., Hess, 1959) since it includes a coefficient accounting for the differences between air and an ideal gas (List, 1966). An equation quadratic in temperature, slightly modified by pressure, describes tabulated values of this coefficient reasonably well. Table 6 lists the algorithm which combines this fit with the defining equation of the mixing ratio.

TABLE 6  
ALGORITHM TO COMPUTE MIXING RATIO

```

FUNCTION WMROF(P,TD)
COMPUTE MIXING RATIO (G/KG)...TEMPERATURE (DEGREES C)...PRESSURE (MB)
T=TD
IF(100.-T) 3,4,4
T=T-273.16
3 CURVE FIT CORRECTION FOR NON-IDEAL GAS
4 X=0.0200*(T-12.5+7500.0/P)
WFW=1.+0.0000045*P+0.00140*X*X
COMPUTE ACCORDING TO STANDARD FORMULA
FWESW=WFW*VAPFW(T)
WMROF=621.97*(FWESW/(P-FWESW))
RETURN
END

```

### 4. HAILSTONE SIZE AND WIND GUST POTENTIAL FROM SOUNDINGS

Prosser and Foster (1966) describe an automated procedure to calculate potential hailstone size and wind gust velocity from operational rawinsonde data. Like most estimates of hailstone size, it is based on updraft speed obtained from an ascending parcel's positive area (see also e.g., Foster and Bates, 1956; Fawbush and Miller, 1953). The wind gust potentials are developed by mixing ascending parcels with environmental air and determining the negative buoyancy as the mixing parcel descends moist adiabatically (see e.g., Foster, 1958; Fawbush and Miller, 1954).

In an effort to determine the utility of these estimates, a verification study was undertaken. Severe thunderstorm reports for the period 01 April to 30 June 1978 were compared with the

TABLE 5  
ALGORITHM TO COMPUTE DEWPOINT

```

FUNCTION DPTOF(EW)
COMPUTE DEWPOINT, DPT, IN DEGREES C GIVEN WATER VAPOR PRESSURE (MB)
CREATE TOLERANCE TO DEGREE DESIRED
TOL=0.00010
IF(EW-0.21382876E-09) 20,20,30
DPTOF = -10000.
RETURN
30 IF(1013.0-EW) 20,100,100
CREATE GUESS BY INVERTING TETEN'S FORMULA
100 X=ALOG(EW/6.1078)
BOT=17.269388-X
DPTOF=(237.3*X)/BOT
BOT=BOT*EW
200 EDP=VAPFW(DPTOF)
CORRECT GUESS BY DERIVATIVE OF TEMPERATURE WITH RESPECT TO VAPOR PRES.
CALCULATED FROM INVERSE OF TETEN'S FORMULA
DTDE=(DPTOF+237.3)/BOT
DELT=DTDE*(EW-EDP)
DPTOF=DPTOF+DELT
CHECK TO SEE IF ANSWER CLOSE ENOUGH, IF NOT ITERATE OVER CORRECTION
IF(ABS(DELT)-TOL)300,300,200
CHANGE SO DEW POINT IS ALWAYS LESS THAN THE TEMP.
COMPATABILITY WITH TOL IS FORCED
300 DPTOF=DPTOF-TOL
RETURN
END

```

nearest rawinsonde-derived predictions as computed from the Prosser and Foster algorithms. Results for wind gusts are shown in Table 7. The first thing to note is that the "preceding" sounding indicated "no gust" potential for more than 60% of the reported severe thunderstorm surface wind gusts (50 kts or greater). When "no gust" cases are excluded, and the reported thunderstorm-associated winds were less than 65 kts, the indicated gust potential was about 6 kt stronger than the observed values. However, for violent gusts (65 kts or greater), even with "no gust" cases excluded, the gust potential computed from preceding soundings was almost 13 kt too slow.

TABLE 7

Less than 65 kt		65 kt or Greater	
Preceding		Preceding	Next
All:	30.5 ± 30.0 (167)	41.3 ± 29.6 (45)	48.1 ± 30.9 (43)
Excl. 0's:	-5.7 ± 6.1 (62)	12.9 ± 8.8 (22)	13.2 ± 10.5 (19)
	105	23	24
105/167 = 62.9% observed gusts 50 ≤ V < 65 kts with 0 calculated (Preceding)			
23/45 = 51.1% observed gusts V ≥ 65 kt with 0 calculated (Preceding)			
24/43 = 55.8% observed gusts V ≥ 65 kt with 0 calculated (Next)			

Table 7. Errors in predicted gust speeds: 01 Apr - 30 Jun 1978, for reported gusts 50 kts or greater in the two categories shown. Values are the mean difference (in knots) of (observed-predicted) ± the associated standard deviation. The number of cases is in parentheses. Values under "Preceding" refer to predictions from the sounding preceding the report by more than 6 hr; whereas "Next" refers to predictions from the sounding immediately following. Values are given for "All" predictions and also excluding cases when the prediction is "no gusts".

Subjectively, the algorithm seems to compute potentials of either about 60 kts or zero. This means that most marginally severe reported gusts (less than 65 kts) are overestimated while really intense windstorms (65 kts or greater) are not forecast. In essence, this technique seems to have relatively little discriminatory skill at estimating wind events.

Observations of hailstone size were substantially in excess of the computed potential (Table 8). "No hail" potential was indicated by the preceding sounding for over 29% of the large hail (3/4 inch or greater) reports. Even with no hail cases excluded, the calculated hail potential was virtually always smaller than the observations. For hail of marginally severe size (less than 2 inches) the average error (excluding zero forecasts) is three-fourths of an inch. Giant hailstones (2 inches or greater) are underestimated by nearly 2 inches (again zeros are excluded). Subjectively, the algorithm rarely finds hail potentials greater than one inch. This technique has little if any ability to discriminate large hail environments from small hail ones.

Because of this, these estimates have been dropped from the NSSFC computerized raob analysis package. In principle, it should be possible to use 1-d cloud models and currently rawinsonde data to predict maximum hailstone size and wind gust speeds more efficiently. In practice, such estimates are less useful than might be expected because of time changes in "environmental" conditions from 12Z to convective development, the inability of the coarse operational radiosonde net to detect mesoscale variations, and the quality of the operational data.

No attempts are currently underway to replace the quantitative estimates of hailstone size and wind gust speeds. Candidates exist, but

in part for reasons already explained, these are not being seriously considered. Further, the physics of large hailstones and strong convective wind gusts appear to be sufficiently complex that algorithms incorporating more detailed physics will not likely repay the effort in an operational context.

TABLE 8

Less than 2 inches		2 inches or Greater	
Preceding		Preceding	Next
All:	0.95 ± 0.64 (449)	2.21 ± 0.85 (70)	2.08 ± 0.85 (71)
Excl. 0's:	0.76 ± 0.62 (317)	1.94 ± 0.73 (51)	1.97 ± 0.93 (54)
	132	19	17
132/449 = 29.4% observed hail $\frac{3}{4}$ ≤ d < 2 inches with 0.0 calculated (Preceding)			
19/70 = 27.1% observed hail d ≥ 2 inches with 0.0 calculated (Preceding)			
17/71 = 23.9% observed hail d ≥ 2 inches with 0.0 calculated (Next)			

Table 8. Errors in predicted hailstone size: 01 Apr - 30 Jun 1978, for reported hailstones  $\frac{3}{4}$  inch or greater, in the two categories shown. Values are the mean difference (in inches) of (observed-predicted) ± the associated standard deviation. The number of cases is in parentheses. See Table 1 for explanation of "Preceding" and "Next". Values are given for "All" predictions and also excluding cases when the prediction is "no hail".

However, a total positive area calculation (Fig. 2) can be useful as an estimate of the maximum possible parcel vertical velocity, and has "replaced" the hailstone size potential in our computerized raob analysis package. Naturally, this parameter's value is limited by the previously mentioned caveats concerning the representativeness of the input data. A negative area is also calculated, which parameterizes the effect of capping inversions (Williams, 1960; Carlson, 1982).

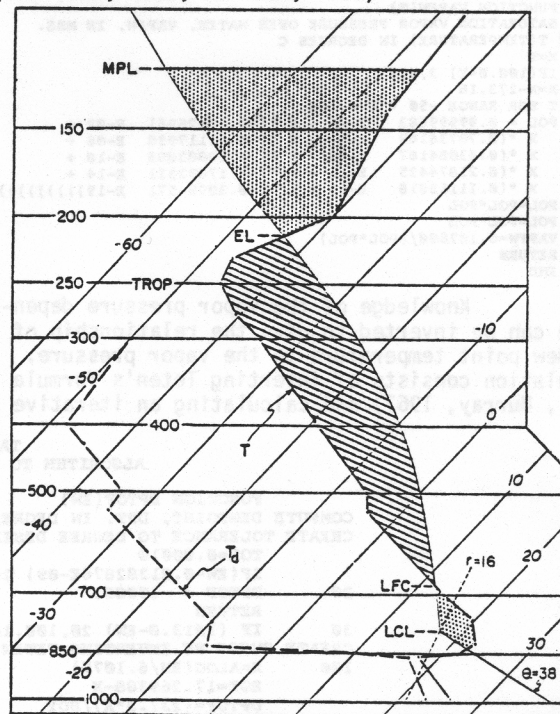


Fig. 2. Sample sounding plotted on skew T-log p diagram, showing parameters as discussed in the text. Hatched region denotes the area where a rising parcel is positively buoyant, while stippling denotes negatively buoyant segments. The dashed line labelled  $r=16$  is a constant mixing ratio, the thin solid line labelled  $\theta=38$  is the dry adiabat used to determine the LCL. The thick solid line labelled  $T$  is the radiosonde ascent curve for temperature, while the dashed, thick line labelled  $T_d$  is that for dew point temperature.



## 5. ESTIMATES OF THUNDERSTORM TOPS FROM SOUNDINGS

Even though parcel theory has limitations, it can be used operationally to interpret the radiosonde data. As shown in Fig. 2, the parcel ascent curve indicates positive buoyancy above the level of Free Convection (LFC). However, the parcel curve eventually re-crosses the raob curve at the Equilibrium Level (EL). As pointed out by Burgess and Davies-Jones (1979), the EL, not the tropopause, is the physically meaningful level for assessing the strength of penetrative convection. Since the EL is most frequently below the tropopause, a severe storm can have large, sustained overshooting of the EL and yet never surpass the tropopause height. Conversely, when the EL is above the tropopause, tops above the tropopause do not necessarily indicate excessively strong storms, since they may not be significantly above the EL. Also, storm anvil clouds should be at or near the EL, rather than the tropopause (as is commonly, and erroneously, assumed).

As overshooting parcels continue to ascend, they subside an increasing negative area (Fig. 2). Pure parcel theory asserts that overshooting parcels will be brought to a halt when the negative area above the EL equals the positive area between the LFC and the EL. Even though this ignores entrainment, forced vertical motion, and so forth, the level which equilibrates the areas above and below the EL ought to give a rough estimate of the maximum height attainable by a parcel through buoyancy in the given sounding. Such a maximum Parcel Level (MPL) approximates the upper bound for thunderstorm tops.

The NSSFC terminal to the University of Wisconsin's McIDAS computer system was used to demonstrate the utility of these concepts. Satellite IR data from 87 storms during May 1981 were used to establish the equivalent black-body temperature ( $T_{BB}$ ) of the storm tops. These values were then related to the nearest preceding rawinsonde observation (Table 9). As anticipated, the mean EL is lower and its temperature is warmer (nearly 5°C) than the mean tropopause temperature. The average observed storm top  $T_{BB}$  was cooler than the mean EL temperature but warmer than the mean tropopause temperature. Also, this  $T_{BB}$  was significantly warmer than the average temperature of the lifted parcel at the MPL. McCann (1982) has found that any thunderstorm whose satellite-observed  $T_{BB}$  approaches or is colder than the EL temperature is hazardous to aviation. It was suggested that a  $T_{BB}$  contour 6°C warmer than the EL outlines the region of greatest aviation hazard.

The appearance of an "Enhanced-V" in contoured satellite IR imagery is often indicative of a severe thunderstorm [e.g., McCann, 1981; Fujita, 1981]. There were 14 enhanced-V storms in the test sample. For these strong storms, the average  $T_{BB}$  was much cooler than for the remaining storms. The derived cloud temperature was, on the average, cooler than the tropopause. It is noteworthy that this tropopause penetration is comparable to the EL overshoot difference for all storms. The dome of the "Enhanced-V" storms is, in the mean, significantly cooler than the EL.

Storm top heights reported by the operational radar network were also obtained for

these storms. These radar-indicated heights, also shown on Table 9, show that the average storm top was higher than both the EL and the tropopause. It is notable that the average storm extended one half (52%) of the way between the EL and the MPL. For the enhanced-V storms, average penetration was much greater.

TABLE 9

	All Storms	Enhanced-V Storms
$T_{sat} - T_{el}$	-4.3	-8.6
$T_{sat} - T_{trop}$	+0.3	-3.7
$T_{sat} - T_{mpl}$	+16.3	+15.3
$H_{ob} - H_{el}$	47	109
$H_{ob} - H_{trop}$	16	73
$H_{ob} - H_{mpl}$	-43	10

Table 9. Temperature (T) differences are given in deg. C, height (H) differences in hundreds of feet.  $T_{sat}$  denotes satellite-derived IR equivalent blackbody temperatures;  $T_{el}$  denotes the radiosonde-derived EL temperature,  $T_{trop}$  the tropopause temperature and  $T_{mpl}$  the MPL temperature.  $H_{ob}$  is the radar-determined storm top height; the rest are heights using notation equivalent to that for temperatures. See text for further discussion.

Extreme caution must be used in the interpretation of all these top data since they are obtained from operational sources, and they are available at half hour intervals at best. Further, the satellite  $T_{BB}$  data are highly dependent upon the satellite's instantaneous field of view (approximately a 10 km square). Adler et al. (1982) show that the satellite-measured  $T_{BB}$  of overshooting storms is about 15°C too warm. Application of such a correction would make the satellite observation of the "all storm" average compatible with the radar data. It penetrates both the EL and the tropopause. Such a correction also makes the relationship between the MPL and the  $T_{BB}$  more reasonable for enhanced-V storms. Note that in the strongest storms, it is possible that within the core of the updraft, pure parcel theory may be more nearly applicable (see e.g., Heymsfield et al., 1978).

Radar echo top heights are also far from perfect. A previous study relating severe weather to radar tops details the caveats pertaining to such data (Darrah, 1978). These, coupled with the assumptions implicit in parcel theory and the effects of temporal modifications in the stratification make the 1,000 ft excess of the radar top over the MPL dubious. Still, it should be noted that the average enhanced-V storm's turret is near the MPL. The observation that the mean "all storm" top is above both the tropopause and the EL is consistent with Darrah's finding that less than 15% of the storms whose radar top lies within the first 8200 ft of the stratosphere are severe. Physically, only these storms which overshoot the EL by a significant amount and maintain this condition for an extended period are likely to be severe.

## 6. SUMMARY

A brief description of the NSSFC computerized rawinsonde analysis package has been presented. Several of the parameters which are computed are examined. It has been shown that both the hail size potential and the wind gust potential have little operational validity. Parcel

theory indicates that positive and negative area and the equilibrium level are the important physical parameters depicting stratification.

*Acknowledgements.* The computer code of tables on through five was initially developed by one of the authors (Hermann B. Wobus) while he was affiliated with the now disestablished Navy Weather Research Facility at Norfolk, Virginia. Typing was skillfully done by Mrs. Beverly Lambert.

#### REFERENCES

- Adler, R.F., M.J. Markus, D.D. Fenn and W.E. Shenk, 1982: Thunderstorm top structure observed by aircraft overflights with an infrared radiometer. Preprints, 12th AMS Conf. Severe Local Storms, Amer. Meteor. Soc., San Antonio, 160-163.
- Barnes, S.L., 1968: An empirical shortcut to the calculation of temperature and pressure at the lifted condensation level. *J. Appl. Meteor.*, **8**, 511.
- Berry, F.A., E. Bollay and N.R. Beers, 1945: *Handbook of Meteorology*, McGraw-Hill, New York, 1068 pp.
- Bolton, D., 1980: The computation of equivalent potential temperature. *Mon. Wea. Rev.*, **108**, 1046-1053.
- Burgess, D.W. and R.P. Davies-Jones, 1979: Unusual tornadic storms in eastern Oklahoma on 5 December 1975. *Mon. Wea. Rev.*, **107**, 451-457.
- Carlson, T.N., 1982: The role of the lid in severe storm formation: Some synoptic examples from SESAME. Preprints, 12th AMS Conf. Severe Local Storms, Amer. Meteor. Soc., San Antonio, 221-224.
- Darkow, G.L. and R.L. Livingston, 1973: Hourly surface static energy analysis as a delineator of thunderstorm outflow areas. Preprints, 9th Conf. on Severe Local Storms, Amer. Meteor. Soc., Denver, 232-237.
- Darrah, R.P., 1978: On the relationship of severe weather to radar tops. *Mon. Wea. Rev.*, **106**, 1332-1339.
- David, C.L. and J.S. Smith, 1971: An evaluation of seven stability indices as predictors of severe thunderstorms and tornadoes. Proc., 7th Conf. on Severe Local Storms, Amer. Meteor. Soc., Kansas City, 105-109.
- Fawbush, E.J. and R.C. Miller, 1953: A method for forecasting hailstone size at the earth's surface. *Bull. Amer. Meteor. Soc.*, **34**, 235-244.
- \_\_\_\_\_, and \_\_\_\_\_, 1954: A basis for forecasting peak wind gusts in non-frontal thunderstorms. *Bull. Amer. Meteor. Soc.*, **35**, 14-19.
- Foster, D.S., 1958: Thunderstorm gusts compared with computed downdraft speeds. *Mon. Wea. Rev.*, **86**, 91-94.
- \_\_\_\_\_, and F.C. Bates, 1956: A hail-size forecasting technique. *Bull. Amer. Meteor. Soc.*, **37**, 135-141.
- Fujita, T.T., 1981: Mesoscale aspects of convective storms. SMRP Res. Paper 191, Dept. of Geophysical Sciences, Univ. of Chicago, 8 pp.
- \_\_\_\_\_, 1982: Infrared, stereo-height, cloud-motion, and radar-echo analysis of SESAME-day thunderstorms. Preprints, 12th Conf. Severe Local Storms, Amer. Meteor. Soc., San Antonio, 213-216.
- Hastings, C., 1955: *Approximations for Digital Computers*. Princeton University Press, Princeton, N.J., 201 pp.
- Hess, S.L., 1959: *Introduction to Theoretical Meteorology*. Holt, Rinehart and Winston, New York, 362 pp.
- Heymsfield, A.J., P.N. Johnson and J.E. Dye, 1978: Observations of moist ascent in Northeast Colorado cumulus congestus cloud. *J. Atmos. Sci.*, **35**, 1689-1703.
- Inman, R.L., 1969: Computation of temperature at the lifted condensation level. *J. Appl. Meteor.*, **8**, 155-158.
- Kreitzberg, C.W., 1964: The structure of occlusions as determined from serial ascents and vertically director radar. Air Force Research Laboratory, Research Report 64-26, Cambridge, Mass., 121 pp.
- List, R.J., 1966: *Smithsonian Meteorological Tables*, 6th Edition, Smithsonian Institution, Washington, D.C., 527 pp.
- Lowe, P.R., 1977: An approximating polynomial for the computation of saturation vapor pressure. *J. Appl. Meteor.*, **16**, 100-103.
- McCann, D.W., 1981: The enhanced-V, a satellite observable severe storm signature. NOAA Tech. Memo. NWS NSSFC-4, National Severe Storms Forecast Center, Kansas City, MO, 31 pp.
- \_\_\_\_\_, 1982: The distribution of severe aviation weather in and near thunderstorms using satellite imagery. Preprints, 12th Conf. Severe Local Storms, Amer. Meteor. Soc., San Antonio, 479-482.
- Murray, F.W., 1967: On the computation of vapor pressure. *J. Appl. Meteor.*, **6**, 203-204.
- Prosser, N.E. and D.S. Foster, 1966: Upper air sounding analysis by use of an electronic computer. *J. Appl. Meteor.*, **5**, 296-300.
- Stackpole, J.D., 1967: Numerical analysis of atmospheric soundings. *J. Appl. Meteor.*, **6**, 464-467.
- Williams, D.T., 1960: The role of a subsidence layer. In "The Tornadoes at Dallas, Tex., April 2, 1957.", Wea. Bur. Res. Paper No. 41 (out of print), 143-158.